Sacher, R., & Ahlquist, P. (1989) *J. Virol. 63*, 4545-4552.
Sgro, J., Jacrot, B., & Chroboczek, J. (1986) *Eur. J. Biochem. 154*, 69-76.
Szilágyi, L., & Jardetzky, O. (1989) *J. Magn. Reson. 83*, 441-449.
Ten Kortenaar, P. B. W., Krüse, J., Hemminga, M. A., & Tesser, G. I. (1986) *Int. J. Pept. Protein Res. 27*, 401-413.
Verduin, B. J. M., Prescott, B., & Thomas, G. J., Jr. (1984) *Biochemistry 23*, 4301-4308.
Vriend, G., Hemminga, M. A., Verduin, B. J. M., de Wit, J. L., & Schaafsma, T. J. (1981) *FEBS Lett. 134*, 167-171.
Vriend, G., Verduin, B. J. M., & Hemminga, M. A. (1986) *J. Mol. Biol. 191*, 453-460.
Wagner, G., & Wüthrich, K. (1982) *J. Mol. Biol. 155*, 347-366.
Wider, G., Lee, K. H., & Wüthrich, K. (1982) *J. Mol. Biol. 155*, 367-388.
Wright, P. E., Dyson, H. J., & Lerner, R. A. (1988) *Biochemistry 27*, 7167-7175.
Wüthrich, K. (1986) *NMR of Proteins and Nucleic Acids*, Wiley, New York.
Wüthrich, K., & Wagner, G. (1979) *J. Mol. Biol. 130*, 1-18.
Wüthrich, K., Wider, G., Wagner, G., & Braun, W. (1982) *J. Mol. Biol. 155*, 311-319.
Wüthrich, K., Billeter, M., & Braun, W. (1984) *J. Mol. Biol. 180*, 715-740.

Reaction of Hydrogen Peroxide with the Rapid Form of Resting Cytochrome Oxidase†

Lichun Weng and Gary M. Baker*
Department of Chemistry, Northern Illinois University, DeKalb, Illinois 60115
Received November 28, 1990; Revised Manuscript Received March 7, 1991

ABSTRACT: The hydrogen peroxide binding reaction has been examined with alkaline-purified resting enzyme in order to avoid mixtures of low pH induced fast and slow conformers. At pH 8.8–9.0 (20 °C), the reactivity of resting enzyme was similar to the peroxide-free, pulsed conformer that has been characterized by other investigators. The reaction showed single-phase reactivity at 435 and 655 nm and required a minimum 8:1 molar excess of peroxide (over cytochrome a_3) for quantitative reaction. At 16:1, the Soret band was stable for 1.0–1.5 h, but above 80:1, the band began showing generalized attenuation within 1–2 min. The peroxide binding reaction was also associated with an increase in absorbance at 606 nm which correlated with the rate of change at 435 and 655 nm. The observed rate constants at each of these wavelengths showed similar linear dependence on peroxide concentration, giving an average bimolecular rate constant of 391 $M^{-1}\cdot s^{-1}$ and a K_d of 5.1 μM. The rise phase at 606 nm was observed to saturate at an 8:1 molar excess of peroxide but showed a slow, concentration-dependent first-order decay that gave a bimolecular rate constant and K_d of 38 $M^{-1}\cdot s^{-1}$ and 20 μM, respectively. The decay was not associated with a change in the Soret absorption or charge-transfer regions, suggesting a type of spectral decoupling. An isosbestic point at 588 nm was consistent with the 606- to 580-nm conversion proposed by other investigators, although direct observation of a new band at 580 nm was difficult. The insensitivity of the Soret band to the loss of absorbance at 606 nm implies that the 606- and 580-nm species do not differ in oxidation state, contrary to the structural assignments made by other investigators. The decay at 606 nm is proposed to be associated with a chemical event at a non-heme site, possibly Cu_B or one of its ligands.

Ligand binding studies of cytochrome *c* oxidase (EC 1.9.3.1) have been complicated by enzyme heterogeneity, particularly in preparations derived from cholate and ammonium sulfate [for recent discussions, see Hartzell et al. (1988), Beinert (1988), and Malmström (1990)]. The reaction of hydrogen peroxide with resting enzyme illustrates the type of problem encountered. For example, a 10-fold molar excess of peroxide was reported by Bickar et al. (1982) to induce only a partial red shift in the Soret band from 417 to 422 nm, but substantial preparation-dependent differences were also observed. Using similar conditions, Vygodina and Konstantinov (1988) observed the band to shift much further, to 427–428 nm. Wrigglesworth (1984) observed a comparable shift, but only with much higher levels of peroxide.

The kinetics in the Soret region also reveal discrepancies. For example, peroxide binding to resting enzyme was shown by Gorren et al. (1986) to consist of a rapid phase followed by a peroxide-independent slow phase, whereas Bickar et al. (1985) have reported three separate phases, each dependent on peroxide concentration.

Variable observations are also evident in the visible region. Witt and Chan (1987) reported a peroxide-induced α-band at 596 nm, whereas other investigators, using either resting or pulsed enzyme, have found this band to be more red-shifted, at 600–601 nm (Bickar et al., 1982; Wrigglesworth, 1984; Kumar et al., 1984a). Complex kinetic patterns associated with peroxide effects on the α-band have also been reported (Kumar et al., 1984a; Bickar et al., 1985).

To find an explanation for these variable effects, we noted that most of the studies cited above were performed at pH

† This investigation was supported by American Heart Association, Illinois Affiliate, Grant C-03 and by Biomedical Research Grant Program Award BRSG S07 RR07176, Division of Research Resources, National Institutes of Health.
* Address correspondence to this author.

0006-2960/91/0430-5727$02.50/0

7.0–7.4. Although this is a typical working pH, it has important implications. In the cases cited above, some of the preparations of resting cytochrome oxidase showed blue-shifted Soret maxima (417–418 nm), for example, Bickar et al. (1982) and Wrigglesworth (1984). Notably, Vygodina and Konstantinov (1988) used a variation of the original Fowler method to prepare their enzyme. This preparation is characterized by a Soret band which is significantly more red-shifted, at 422–424 nm (Muijsers et al., 1971; Hartzell et al., 1978). Cytochrome oxidase, prepared by a modification to the Hartzell and Beinert approach, will also exhibit a Soret band at 422–424 nm, as long as the pH is maintained sufficiently high during the soluble stages of enzyme purification (Baker et al., 1987; Papadopoulos et al., 1991). In this alkaline state, the enzyme displays rapid, monophasic reactivity with cyanide, similar to that observed in redox-cycled preparations. Exposure of resting enzyme to low pH (<8.5) causes the Soret band to blue-shift and converts the enzyme to a form that shows 50–100-fold slower reactivity with cyanide (Baker et al., 1987). Variable mixtures of fast and slow forms can be present since the extent of these effects is dependent both on the time of incubation and on the acutal pH.

These complications of low pH have prompted us to examine the hydrogen peroxide reaction under alkaline conditions, where no conversion to the slow conformer occurs. The results establish that the reaction of resting enzyme with hydrogen peroxide is similar to that of the pulsed preparation originally reported by Kumar et al. (1984b). Additionally, the use of resting enzyme to follow peroxide binding has allowed observation of a series of spectral and kinetic correlations that have not been previously documented. The results are discussed in the context of the peroxy/oxyferryl model proposed by Witt and Chan (1987).

Materials and Methods

Enzyme Purification and Characterization. Cytochrome *c* oxidase was purified from bovine heart as described by Baker et al. (1987). The method involves a series of minor modifications to the original procedure of Hartzell and Beinert (1974). The pH during the soluble stages of purification was monitored with a pH electrode and maintained at 8.8–9.0 (4–6 °C) with 3 N KOH. The final precipitate was dispersed in cold buffer containing either 50 mM KH_2PO_4·KOH or 50 mM 2-(*N*-cyclohexylamine)ethanesulfonic acid·potassium hydroxide (CHES·KOH)[1] and 0.1% (w/v) *n*-dodecyl β-D-maltoside (DM) at pH 9.0 (20 °C). Stocks of 700–900 μM heme *a* were then stored in liquid nitrogen until use. Heme *a* concentration was determined by measuring the absorbance of the reduced α-band at 604 nm and applying an extinction coefficient of 20.9 $mM^{-1}·cm^{-1}$ [averaged from Brunori et al. (1979) and Yonetani (1960)]. The concentration was also checked against the value obtained by using an extinction coefficient appropriate for the position of the oxidized Soret band (i.e., 78 $mM^{-1}·cm^{-1}$ at λ_{max} = 423 nm; Papadopoulos et al., 1991). The average uncertainty in actual heme *a* concentration was ≤10%. Specific buffer conditions are indicated in the figure legends.

Activity was assayed in 0.1 M potassium phosphate buffer and 0.1% (w/v) DM at pH 6.0, 20 °C, according to the method of Yoshikawa et al. (1977). The maximal turnover number, calculated from observed rate constant data over a range of cytochrome c^{2+} concentrations (6–25 μM), was generally 250 μM cyt $c^{2+}·s^{-1}·\mu M^{-1}$ heme *a*, somewhat higher than the value of 180 s^{-1} reported by Hartzell and Beinert (1974). Total bound phosphorus, determined by a modification of the method of Chen et al. (1956), was 4.5–6.0 nmol of P/nmol of heme *a*, consistent with the 2–5 nmol of P/nmol of heme *a* range reported by Hartzell et al. (1978). Phosphorus determinations were performed on enzyme stocks that were dispersed in CHES/DM buffer. Heme *a* content was 8.5–9.0 nmol of heme *a*/mg of protein, and was based on the original protein assay method of Lowry et al. (1951).

Ligand Binding Kinetics. Sodium cyanide stocks at 4 M were freshly prepared in water and partially neutralized with 6 M HCl to give a final pH of 8.8 at 20 °C. An aliquot was mixed with a 5 μM heme *a* solution (at either pH 6.8 or pH 8.8, 20 °C), giving a final, calculated cyanide concentration of 25 mM.

Hydrogen peroxide stocks (Fisher, assay w/w, 30.0–32.0%) were checked periodically by using the ceric sulfate method of Kolthoff and Belcher (1957). Serial dilutions were made just prior to the experiment to give 1.668–166.8 mM concentrations, which were then used for addition to heme *a* solutions at either pH 6.8 or pH 8.8–9.2, 20 °C.

Cyanide and hydrogen peroxide stocks were maintained on ice. The low-pH ligand binding experiments were performed by diluting the enzyme stock into buffer containing 50 mM KH_2PO_4·KOH, 167 mM K_2SO_4, and 0.1% (w/v) DM (pH 6.8, 20 °C). Mixing times for all time scans prior to data acquisition was 10–15 s.

Instrumentation and Data Analysis. Wavelength and time scans were recorded with a PC-interfaced Shimadzu UV-3000 spectrophotometer equipped with a magnetic stirrer and constant temperature regulation. Spectra were collected in double-beam mode using 50 nm/min and ±0.2-nm resolution. Kinetic scans were either double-beam (435, 655 nm) or dual-wavelength (606 minus 625 nm) and reflect data points every 1–2 s. Spectral and arithmetic processing (subtraction and smoothing) relied on Lab Calc (Galactic Industries Inc., Salem, NH). Symbol plots and nonlinear curve fitting were accomplished with SigmaPlot 4.0 (Jandel Scientific, Corte Madera, CA). All graphics displays were prepared with an HP LaserJet III printer at 300 dpi.

Results

Effect of Hydrogen Peroxide on the Soret Band of Resting Enzyme. A series of spectra recorded at 1-min intervals following the addition of 20 μM hydrogen peroxide is shown in Figure 1A. At pH 9.0, the Soret band intensified and shifted within several minutes from 424 to 428 nm. The isosbestic point at 425 nm is consistent with a simple, two-state conversion of unreacted cytochrome a_3 into product. Figure 1B shows the corresponding exponential time course of the absorbance increase at 435 nm (the wavelength of maximal change). At 40 μM peroxide, the absorbance at kinetic saturation remained stable over 1.5 h of incubation, decreasing by less than 5% (data not shown).

The peroxide binding kinetics in Figure 1B show that single-phase reactivity is not unique to cyanide, although much higher concentrations of cyanide are required to give the same observed rate. Table I extends the ligand comparison to low pH. Experiment 1 represents the pH 9.0 control case where each ligand showed 100% fast reactivity. To promote conversion to the slower reactive form(s), resting enzyme was titrated to pH 6.8–7.4 and incubated for 2 and 6 h at 20 °C (experiments 2 and 3, respectively). The binding kinetics were measured for each ligand, and the procedure described in the table legend was used to extract the percentage of fast component. Table I shows that low pH affected cyanide and

[1] Abbreviations: CHES, 2-(*N*-cyclohexylamino)ethanesulfonic acid; DM, *n*-dodecyl β-D-maltoside.

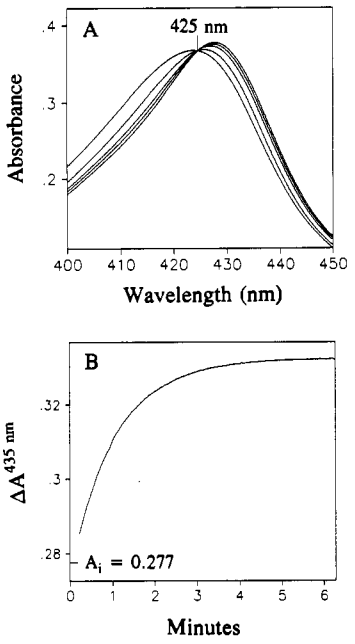

FIGURE 1: Time-dependence of an 8:1 molar excess of hydrogen peroxide on the Soret band of resting cytochrome oxidase. (A) Resting enzyme was incubated at pH 9.0, 20 °C, for 1 h to allow equilibrium of the Soret band position to 423.7 nm (the most blue-shifted spectrum shown in the figure). Hydrogen peroxide (standardized as described under Material and Methods) was transferred into a solution of 5.0 μM heme a(±5%) at pH 9.0, 24 °C, to give a final concentration of 20 μM (8:1 molar excess over cytochrome a_3). The buffer consisted of 0.1 M KH_2PO_4·KOH, 167 mM K_2SO_4 (μ = 0.5 M, excluding contribution from P_i), and 0.1% (w/v) n-dodecyl β-D-maltoside (DM). After a 10-s mixing time, four spectra were recorded at 1-min intervals. (B) The time course associated with the addition of 40 μM hydrogen peroxide was measured at 435 nm at pH 9.0, 20 °C, using the buffer system described above. Mixing time prior to data acquisition was 15 s.

hydrogen peroxide binding comparably, with longer incubation times promoting further conversion in each case.[2]

Figure 2 compares several spectra, obtained at pH 9.0, following the addition of different concentrations of hydrogen peroxide, from 2.5 to 200 μM. For proper comparison, each spectrum was recorded at the point of kinetic saturation. At a 1:1 and 2:1 molar ratio with cytochrome a_3 (2.5 and 5.0 μM peroxide), the Soret band had not fully shifted to 428 nm. A minimum of 20 μM peroxide was needed for quantitative reaction since higher concentrations, up to 200 μM after 10 min, showed no further changes in the spectrum. An isosbestic point at 425 nm was again evident. Above 200 μM peroxide, there was initially slight but progressive attenuation of the near-UV absorption envelope, suggesting nonspecific heme bleaching.

Effect of Hydrogen Peroxide on the Visible Region of Resting Enzyme. Figure 3 shows the effect of 2.5–20 μM peroxide on the 655-nm charge-transfer band. In accord with Figure 2, a minimum peroxide concentration of 20 μM (Figure 3, trace d) was needed for kinetic saturation, indicating reversible binding. Exponential fits corresponding to each trace are also shown. Extrapolation of each curve to infinite time gave final absorbance values that were also consistent with an approach to an equilibrium state.

Figure 4A shows the effect of cumulative additions of hydrogen peroxide, from 20 μM to 1.5 mM, on the α/β-band region of resting enzyme. An 8:1 molar excess (20 μM) caused the α-band to intensify and shift slightly to 601 nm. The charge-transfer band at 655 nm was eliminated and the trough absorbance, centered at 570 nm, intensified. Continued additions of peroxide caused the α-band to lose amplitude and shift back to the blue, eventually stabilizing at 597 nm. The loss did not reflect restoration of the resting conformer since the 655- and 428-nm bands remained unchanged. Isosbestic points were observed at 625 and 588 nm. The blue region

Table I: Reactivity of Resting Enzyme with Cyanide and Hydrogen Peroxide following Exposure to Low pH

	CN^- binding		H_2O_2 binding	
expt[a]	% fast[b]	% remaining[c]	% fast[b]	% remaining[c]
1	100	0	100	0
2	41	59	41	59
3	22	78	23	77

[a] Addition of ligand (either 25 mM NaCN or 40 μM H_2O_2) to a 5 μM heme a solution occurred after the following treatment conditions: experiment 1, 1 h of incubation at pH 8.8, 20 °C; experiment 2, sample was diluted into pH 6.8 buffer and incubated 2.3 h at 20 °C; experiment 3, same as experiment 2 except that the incubation time at pH 6.8 was 6 h. Buffer composition at pH 8.8 was as in Figure 1 (CHES/DM was also used in separate experiments). The low-pH buffer composition is given under Materials and Methods. Potassium sulfate was included to prevent turbidity at pH values below 7. [b] k_{obs} was 0.02–0.04 s^{-1}. [c] This percentage includes slow and unreactive components. Estimation of the final absorbance of the fully reacted state (in order to obtain an accurate value for the percentage of rapid conformer) required the use of an extinction coefficient corresponding to the incubation pH. This was determined by adding cyanide or hydrogen peroxide after 30 s following titration to pH 6.8, 20 °C. The 30 s is insufficient time for fast to slow (or unreactive) conversion to occur. The intrinsic effect of pH on the amplitude of the CN^- or H_2O_2 binding reaction is thereby determined without the complications of low pH induced heterogeneity. Details of this approach will be published elsewhere.

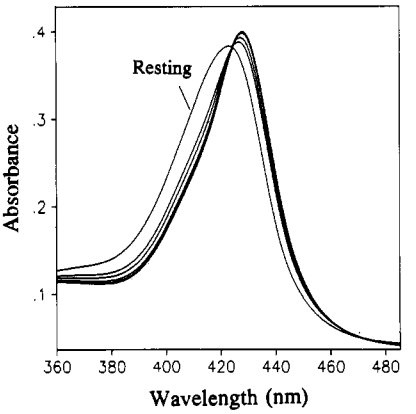

FIGURE 2: Effect of hydrogen peroxide concentration on the equilibrium Soret band position of resting cytochrome oxidase. A 5.0 μM heme a solution was prepared as in Figure 1A except that 0.1 M CHES was used instead of phosphate and the pH was 9.2 at 20 °C. A different preparation of enzyme was used in this case, and after 1 h of incubation, the Soret band position was at 422.7 nm rather than the 423.7 nm shown in figure 1A (resolution = ±0.2 nm). After the 1-h equilibration period, hydrogen peroxide was added in separate experiments to give 2.5, 5.0, 20, 60, 100, and 200 μM final concentration. Each spectrum shown was recorded at the point of kinetic saturation and normalized to a heme a concentration of 5.0 μM.

[2] Some preparations have shown a further complication after overnight exposure to low pH (<7). Addition of 20 μM peroxide resulted in a single phase of reactivity, but at the point of kinetic saturation, the amplitude of the change was unusually small, and the Soret maximum had only partially shifted, to 425–426 nm. Further additions of peroxide (up to 1 mM) simply caused a loss of Soret band amplitude without any further red shift, implying an unreactive population of a_3 centers. Bickar et al. (1982), working at pH 7.4–7.5, had also noted preparation-dependent variations in the proportion of cytochrome a_3 centers that bound hydrogen peroxide, which very likely reflects the type of low pH induced heterogeneity described here.

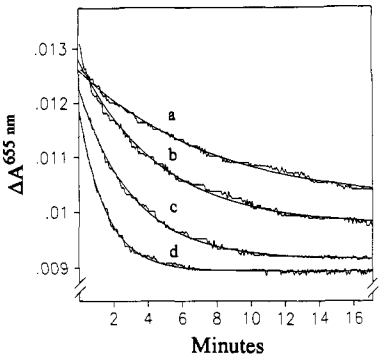

FIGURE 3: Kinetics of the absorbance change at 655 nm following the addition of hydrogen peroxide. Hydrogen peroxide was added to a 5.0 μM heme *a* solution at pH 9.0, 20 °C, to give final concentrations of 2.5 (a), 5.0 (b), 10 (c), and 20 μM (d). Buffer conditions were as in Figure 2. In each case, data acquisition at 655 nm began after a 13-s mixing time. The raw data were smoothed by Savitsky–Golay convolution and fit with a single exponential to extract an empirical rate constant. Curve fits are shown in each case as solid lines.

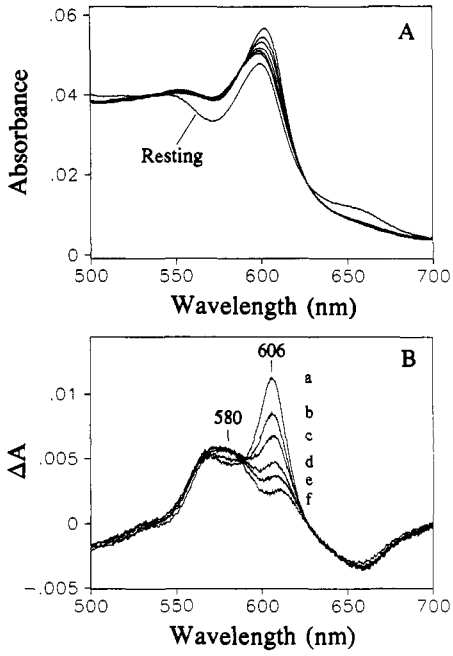

FIGURE 4: Effect of cumulative additions of hydrogen peroxide on the visible spectrum of resting enzyme. (A) Buffer conditions and pH were as in Figure 1A. Hydrogen peroxide was added incrementally to a 5.0 μM heme *a* solution at 20 °C to give cumulative final concentrations of 20, 80, 160, 260, 860, and 1460 μM. The α-band showing the largest intensity represents the lowest concentration case (20 μM). Further additions of peroxide resulted in a progressive loss of amplitude. A wavelength scan was initiated 13 s after addition of hydrogen peroxide, and the time interval between the start of successive scans was 11 min. The resting spectrum is shown for comparison. (B) The resting spectrum shown in (A) was subtracted from each of the peroxide-treated cases to give the difference spectra labeled a–f, with spectrum a corresponding to the 20 μM case.

below 588 nm showed only very minor changes as the peroxide concentration was increased to 1.5 mM.

Figure 4B shows a series of difference spectra obtained by subtracting resting enzyme from each of the peroxide-treated cases in Figure 4A. The lowest concentration of peroxide (trace a, 20 μM) revealed a prominent transition at 606 nm and a weak transition at 570 nm, essentially the features that Wikström (1981) originally assigned to the "peroxy" form of cytochrome a_3. The further addition of peroxide caused the 606-nm band to lose intensity and shift to 610 nm, although it cannot be determined whether this was an actual shift or

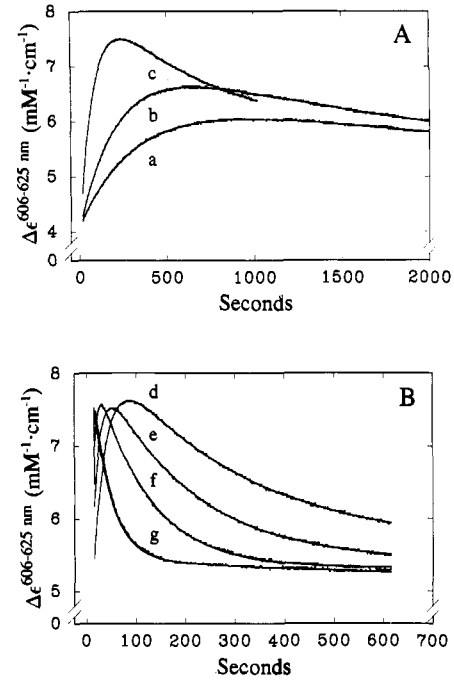

FIGURE 5: Kinetics of the peroxide-dependent absorbance change at 606 nm. (A) Buffer conditions were as in Figure 1A. Hydrogen peroxide was added in separate, sequential experiments to a 5.0 μM heme *a* solution at pH 9.0, 17 °C, to give 2.5 (a), 5.0 (b), and 20 μM (c). Time scans were recorded in the dual-wavelength mode by measuring $\Delta A^{606-625\ nm}$. The mixing time prior to the first data point was 13 s in each case. The observed traces were fit with a two-exponential equation ($A = A_d e^{-k_{obs,d}t} - A_r e^{-k_{obs,r}t} + C$) and are shown overlaid with the raw data. The equation subscripts r and d refer to the rise and decay phases, respectively. (B) Treatment conditions were as in (A) except that the following hydrogen peroxide concentrations were used: 60 (d), 100 (e), 200 (f), and 600 μM (g). Nonlinear least-squares fits based on the sum of two exponentials are overlaid on traces d–f, as in (A). For trace g, the rise phase was over within the 13-s mixing time, and the decay could not be fit with a single exponential. A linear slope was used to approximate the amplitude of the slower component.

simply the result of a weaker, underlying transition. A slight increase at about 580 nm was also evident, which caused some broadening, but the observed increase was not correlated with the incremental loss of amplitude at 606 nm. The absorbance at 580 nm remained essentially unchanged as the peroxide concentration was increased above 160 μM (traces c through f). The largest change at 580 nm occurred at the lowest peroxide concentration (20 μM, trace a), where the 606-nm band was still very prominent. Peroxide concentrations in excess of 1.5 mM showed continued loss of amplitude at 606 nm and a less progressive loss at 580 nm. The resulting spectra no longer displayed the isosbestic point at 588 nm (not shown).

Figure 5A,B shows the rise and decay kinetics of the 606-nm transition for seven different peroxide concentrations within the range 2.5–600 μM. (It becomes difficult above 600 μM to fully capture the decay phase without stopped-flow monitoring.) The amplitude of the rise phase was independent of peroxide concentration at $\geq$20 μM (traces c through g), indicating essentially quantitative formation of the 606-nm species ($\Delta\epsilon^{606-625nm}$ was estimated at 3.3 $mM^{-1}\cdot cm^{-1}$). The slower decay phase appeared to saturate at $\geq$200 μM peroxide (traces f and g). However, the 600 μM decay (trace g) could not be fit with a single exponential (see figure legend), identifying the onset of a slower component that became more prominent at higher peroxide concentrations (data not shown). Comparison of the difference spectrum recorded at the end of the 600 μM decay phase with those in Figure 4B (where

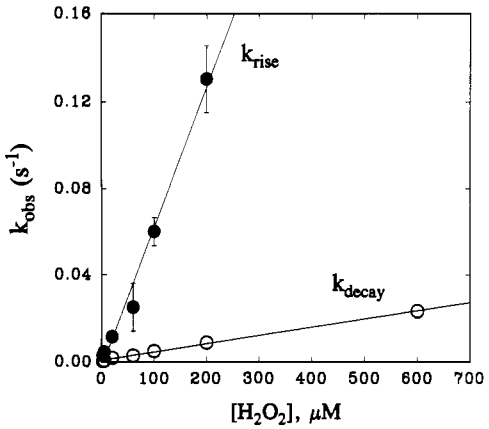

FIGURE 6: Peroxide concentration dependence of the observed rate constants for the rise and decay phases at 606 nm. Observed rate constants were extracted from time scan data of the type shown in Figure 5A,B. Data averaged from three enzyme preparations were used to calculate the standard error bars.

the peroxide concentration range was extended to 1.5 mM) showed that the 606-nm band amplitude had only partially decayed. Continued loss of the 606-nm intensity becomes measurably biphasic at peroxide concentrations ≥600 μM, and is consistent with the biphasic decay that other investigators have observed using 1–2 mM peroxide (Kumar et al., 1984a; Bickar et al., 1985). The slower component did not interfere with the difference absorption profile since retention of the isosbestic point at 588 nm was observed at peroxide concentrations as high as 1.5 mM (figure 4A).

The empirical rate constants for each trace in Figure 5A,B were extracted from two-exponential curve fits (except trace g) and plotted against peroxide concentration in Figure 6. The standard error bars reflect kinetic results for three different enzyme preparations. The linear dependence of each phase on peroxide concentration gave bimolecular rate constants of 644 and 38 $M^{-1}\cdot s^{-1}$ for the rise and decay phases, respectively.

The red shift to 428 nm and the elimination of the 655-nm band were shown in Figures 2 and 3 to require an 8:1 molar excess of peroxide. These data imply that the peroxide binding reaction is reversible and should therefore produce a nonzero ordinate intercept in a plot of the type shown in Figure 6. To estimate this value, the observed rate constants at 435, 606 (rise phase), and 655 nm were plotted against peroxide concentration on an expanded scale, from 0 to 60 μM. The k_{obs} values showed similar dependence on peroxide concentration at each wavelength (data not shown), suggesting that the same structural event was being measured. Linear regression of the entire data set resolved a nonzero intercept corresponding to an equilibrium dissociation constant (K_d) of 5.1 μM, in accord with estimates from other investigators [for example, Bickar et al. (1982) and Vygodina and Konstantinov (1987)]. The slope of the data, using the combined data sets, gave a bimolecular rate constant of 391 $M^{-1}\cdot s^{-1}$, which is substantially different than the value of 644 $M^{-1}\cdot s^{-1}$ observed in Figure 6 for the rise phase at 606 nm. The lower value may be more representative since it averages the contributions at three different wavelengths and reflects a range of peroxide concentrations for which curve-fitting variations are minimal (see legend to Figure 6). Low ionic strength buffer (50 mM CHES·KOH, rather than the KP_i/K_2SO_4 buffer described in the legend to Figure 1) was also used to obtain preliminary measurements of k_{obs} at 435 nm. The same exponential behavior was evident over a range of peroxide concentrations, but a somewhat higher value for the bimolecular association constant was noted.

The decay-phase at 606 nm (extracted from Figure 5A,B) gave a K_d of 20 μM when plotted over the 0–600 μM peroxide concentration range. (Curve-fitting variations for these data were minimal, as evidenced by the small standard error bars shown in Figure 6.)

Discussion

The heterogeneous response of resting enzyme to ligands such as hydrogen peroxide and cyanide can be prevented by maintaining the pH sufficiently high (>8.5) during the purification and subsequent dilution of stock preparations (Baker et al., 1987; Papadopoulos et al., 1991). Table I demonstrates the ligand binding complications caused by exposure of resting enzyme to low pH. Slow or unreactive conformers[2] become evident in proportions that increase as the pH is lowered and the incubation time is extended. These results suggest that the variable peroxide (and cyanide) binding behavior observed by different investigators (see the introduction) is very likely due to differences in pH and exposure time prior to the addition of ligand. The use of alkaline conditions has permitted an evaluation of the intrinsic heterogeneity of the peroxide reaction without interference from low pH dependent conformers. Although it can be argued that the same advantage applies to redox-cycled preparations, it is our opinion that other complications have arisen due to the chemical complexity of the reaction mixtures and the use of large excesses of hydrogen peroxide.

The reaction of hydrogen peroxide with resting enzyme (pH 8.8) has the following characteristics: The Soret band shifts from 423–424 to 428 nm (Figures 1A and 2) and requires a minimum 8:1 molar excess (over cytochrome a_3) for quantitative reaction (Figures 2 and 3). The shift occurs as a single, exponential phase (Figure 1B) and is associated with an average bimolecular rate constant of 391 $M^{-1}\cdot s^{-1}$ (see Results). Similar peroxide binding behavior has been observed at pH 7.0 with the redox-cycled (pulsed) enzyme originally described by Kumar et al. (1984b). However, the peroxide adduct observed by Chance and co-workers is much less stable, with decay commencing in minutes rather than hours. The Soret band positions of the pulsed and resting forms are also different: 420 nm for the pulsed compared with 423–424 nm for the resting. Titration of resting enzyme from pH 8.8 to about 7.5 will shift the Soret band to 420 nm (Papadopoulos et al., 1991), but after several minutes of incubation, the enzyme invariably shows mixtures of the fast and slow ligand binding forms. These considerations suggest that the pulsed preparation is somehow structurally different. However, Gorren et al. (1986), using the Fowler method of enzyme preparation (see the introduction), have found the band position of their pulsed enzyme to be more red-shifted than that reported by Kumar et al. (1984b), 424 nm rather than 420 nm. The reason for this discrepancy is not clear, but taken together, the results imply that resting enzyme derived from alkaline purification is structurally similar to the pulsed (peroxide-free) state, as originally suggested by Baker et al. (1987). It is also this form of the enzyme that appears to be associated with the mitochondrial inner membrane (Baker et al., 1987).

The homogeneous binding behavior observed for the Soret and charge-transfer bands is not observed in the α/β absorption region. Hydrogen peroxide causes the α-band to intensify and shift slightly to the red, from 598 to 601 nm. However, even at stoichiometric concentrations with cytochrome a_3, the band amplitude is not stable and is observed to decay (Figure 5A). At very high concentrations (≥1.5 mM), the α-band continues to lose amplitude and blue-shifts to 596–597 nm (Figure 4A). Difference spectra show that the loss of amplitude is associated

with an absorbance decrease at 606 nm (Figure 4B) with only slight changes evident at other wavelengths. Several investigators, however, have reported difference spectral features at 606 and 580 nm, with the relative proportions depending on the peroxide concentration. The 606-nm (or "peroxy") form is prominent at low concentrations (Wrigglesworth, 1984; Vygodina & Konstantinov, 1988) whereas the 580-nm form, described by Witt and Chan (1987) as an oxyferryl derivative of cytochrome a_3, predominates at higher concentrations. The implication is that the loss of the 606-nm band, which has generally been associated with millimolar concentrations of peroxide, should correlate to an increase in absorption at 580 nm. However, the spectral and kinetic relationships between the two forms have not been clearly documented.

Examination of the difference spectra in Figure 4B shows that the peroxide-dependent loss at 606 nm does not readily correlate with the appearance of a new peak at 580 nm, which is contrary to the proposed conversion. However, the occurrence of an isosbestic point at 588 nm (Figure 4B) is not consistent with a continued loss of absorbance at 606 nm unless there is a compensating increase on the high-energy side of the isosbestic point. It is therefore possible that increased levels of peroxide cause both α- and β-bands (at 606 and 570 nm) to lose amplitude and that a compensating increase occurs at about 580 nm which leaves the absorbance at that wavelength only slightly enhanced (Figure 4A,B). Nonetheless, the prominence of a band at 580 nm at high peroxide concentrations is the net result of lost amplitude at 606 nm without much apparent increase at 580 nm. The new transition at 580 nm is expected to correlate to an increase at 535 nm (Orii & King, 1976; Witt & Chan, 1987). Careful inspection of the spectra in Figure 4B is consistent with this, although quantitation from the data shown is difficult.

The use of high concentrations of hydrogen peroxide has caused some confusion. Wrigglesworth (1984), using heterogeneous resting enzyme, suggested that the shift of the Soret band to 428 nm was associated with the formation of the 580-nm transition. Witt and Chan (1987) have accordingly referred to a 428/580-nm species, implying a possible relationship between these band positions. Kumar et al. (1984a) have associated the 580-nm band with a loss of the 655-nm charge-transfer band. However, at low enough peroxide concentrations, it becomes clear that the absorbance changes at 435 and 655 nm correlate to the rise phase of the 606-nm band, and not to its decay. It thus becomes appropriate to refer to 428/606- and 428/580-nm forms, the former being relatively unstable, even at stoichiometric concentrations of peroxide (Figure 5A, trace a).

A simple kinetic mechanism that accounts for the peroxide binding data is

$$[a_3(\mathrm{III})\text{–X–}\mathrm{Cu_B(II)}] + \mathrm{H_2O_2} \underset{k_{-1}}{\overset{k_1}{\rightleftharpoons}} [428/606\ \mathrm{nm}] \quad (1)$$

$$[428/606\ \mathrm{nm}] + \mathrm{H_2O_2} \underset{k_{-2}}{\overset{k_2}{\rightleftharpoons}} [428/580\mathrm{nm}] \quad (2)$$

The bimolecular rate constants, k_1 and k_2, are 391 and 38 $M^{-1}\cdot s^{-1}$, respectively, and the dissociation constants, K_d, for eq 1 and 2 are 5.1 and 20 μM (see Results). The value of 5.1 μM for eq 1 is consistent with the minimum 8:1 molar excess that is required to saturate the absorbance change at 435, 606, and 655 nm (Figures 2, 4, and 6). It is also consistent with the ability of catalase to partially reverse the peroxide-induced spectral changes (Vygodina & Konstantinov, 1988). The model suffices for conditions that allow retention of the isosbestic point at 588 nm (Figure 4B). At very high peroxide concentrations (>1.5 mM), the isosbestic wavelength is no longer evident, reflecting more complicated changes.

Establishing correlations between the visible and Soret region has important implications for structure. The 580-nm species is proposed to be similar to the ferryl porphyrin known to be present in horseradish peroxidase (HRP) compound II (Wikström, 1987; Chan et al., 1988; Kumar et al., 1988), whereas the 606-nm species is generally viewed as a peroxy derivative of ferric cytochrome a_3. The problem with this assignment is that the change in oxidation state associated with the 606- to 580-nm conversion, from Fe(III) to Fe(IV), cannot be easily reconciled with the observed stability of the Soret band during conditions that promote both a rise and a decay of the 606-nm difference feature. For example, at 40 μM peroxide, the absorbance change at 435 nm shows first-order saturation within a few minutes of incubation, with only a slight decrease in absorbance over 1.5 h (see text for Figure 1). Yet, within minutes, the 606-nm band begins to show significant decay (Figure 5A). Furthermore, after 10 min of incubation, the Soret envelope at 200 μM peroxide is identical with that at 20 μM (Figure 2), despite a substantial difference in the amount of decay at 606 nm (compare traces c and f in Figure 5A,B after 600 s). Comparisons above 200 μM peroxide are difficult since the Soret band begins to show generalized attenuation, but the band position remains at 428 nm.

These data clearly show that the Soret band red-shifts to 428 nm prior to any significant conversion to the 580-nm species, in accord with recent peroxide binding results in vesicles reconstituted with cytochrome oxidase (Vygodina & Konstantinov, 1988). Studies of the superoxide reaction with iron porphyrins (McCandlish et al., 1980) show that the red shift in the Soret band is consistent with the proposed structure of the 606-nm form, namely, a high-spin Fe(III)–peroxy complex. However, during the subsequent decay at 606 nm, the Soret envelope remains unchanged in every aspect (shape, amplitude, center frequency), a result that seems surprising if that decay is associated with a ferric to ferryl transition. For example, HRP·II shows a Soret band position that is red-shifted compared with the native ferric heme state, 420 nm instead of 403 nm (Hewson & Hager, 1979). In cytochrome *c* peroxidase (CcP), both compounds I and II are ferryl porphyrin and show very similar Soret spectra (the radical in CcP·I resides on an amino acid). The native ferric heme is at 408 nm, and the ferryl derivatives are both at 419 nm (Yonetani, 1965; Ho et al., 1983).

A structural model for the 606- and 580-nm forms must be consistent with the observation that the 580-nm form is 1 oxidizing equiv above the native ferric state, probably due to ferryl porphyrin, and also that the 606-nm form lies 1 oxidizing equiv above the 580-nm state (Wikström, 1981, 1987). Accordingly, it becomes appropriate to view the 606- and 580-nm species as structural analogues of CcP compounds I and II. An amino acid radical, possibly associated with a ligand to Cu_B, would characterize the 606-nm state and would be quenched by excess peroxide during the decay into the 580-nm form. The difference extinction coefficient associated with the monophasic decay at 606 nm is about 2.2 $mM^{-1}\cdot cm^{-1}$ (traces f and g, Figure 5B) and corresponds to the approximate position and amplitude of the tryptophan radical proposed for CcP·I (Ho et al., 1983). The formation of an amino acid radical would essentially follow the scheme already proposed by Chan et al. (1988) to explain the 606- and 580-nm forms. Homolytic cleavage of a bridging peroxy bond (presumed to form within the 10–15-s mixing time of our kinetic experiments) would result in oxyferryl, leaving oxygen-ligated

Cu_B(II) with an unpaired electron on the oxygen. Oxidation of a nearby amino acid residue (possibly a tryptophan) would quench the oxygen radical, leaving hydroxylated Cu_B(II). Our data would indicate that the 606- and 580-nm forms are both ferryl porphyrin, analogous to CcP·I and ·II, whereas in the model proposed by Chan et al. (1988) only the 580-nm form is ferryl. Since the 606-nm decay involves only the radical site (or possibly the Cu_B site), and not the cytochrome a_3 center, the Soret absorption envelope remains unchanged during the 606- to 580-nm transition. Detection of the radical is anticipated to be difficult because of spin coupling and its inherent instability, especially at high peroxide concentrations. A further difficulty is that radical quenching does not readily account for the appearance of new absorption bands at 580 and 535 nm, although reference to Figure 4A,B shows that the principal absorbance change is simply a loss of α-band intensity without much correlated change at other wavelengths. A structural model must also be compatible with the reversibility shown in eq 1 and 2. It is also interesting to note that Malmström and co-workers (Clore et al., 1980) proposed a ferryl–a_3 structure for what they termed compound III_M (analogous to Chance's compound C). Compound III_M was obtained by reaction of two-electron-reduced cytochrome oxidase with oxygen. Whatever the real explanation, the results presented here, particularly Figure 5A,B, establish experimental guidelines for the application of rapid detection spectroscopy, such as EPR and resonance Raman, that can test the above proposal and possibly clarify the structural identity of the 606- and 580-nm forms.

ACKNOWLEDGMENTS

We are grateful to Professor James Erman for a critical review of the manuscript and to Professor Graham Palmer for helpful discussions on the kinetics of the peroxide binding reaction. We also thank the reviewers of the manuscript for their helpful comments.

Registry No. H_2O_2, 7722-84-1; cytochrome oxidase, 9001-16-5.

REFERENCES

Baker, G. M., Noguchi, M., & Palmer, G. (1987) *J. Biol. Chem. 262*, 595–604.

Beinert, H. (1988) *Chem. Scr. 28A*, 35–40.

Bickar, D., Bonaventura, J., & Bonaventura, C. (1982) *Biochemistry 21*, 2661–2666.

Bickar, D., Lehninger, A., Brunori, M., Bonaventura, J., & Bonaventura, C. (1985) *J. Inorg. Biochem. 23*, 365–372.

Brunori, B., Colisimo, A., Rainoni, G., Wilson, M. T., & Antonini, E. (1979) *J. Biol. Chem. 254*, 10769–10775.

Chan, S. I., Witt, S. N., & Blair, D. F. (1988) *Chem. Scr. 28A*, 51–56.

Chen, P. S., Toribara, T. Y., & Warner, H. (1956) *Anal. Chem. 28*, 1756–1758.

Clore, G. M., Andrêasson, L.-E., Karlsson, B., Aasa, R., & Malmström, B. G. (1980) *Biochem. J. 185*, 155–167.

Gorren, A. C. F., Dekker, H., & Wever, R. (1986) *Biochim. Biophys. Acta 852*, 81–92.

Hartzell, C. R., & Beinert, H. (1974) *Biochim. Biophys. Acta 368*, 318–338.

Hartzell, C. R., Beinert, H., Van Gelder, B. F., & King, T. E. (1978) *Methods Enzymol. 53*, 54–66.

Hartzell, C. R., Beinert, H., Babcock, G. T., Chan, S. I., Palmer, G., & Scott, R. A. (1988) *FEBS Lett. 236*, 1–4.

Hewson, W. D., & Hager, L. P. (1979) *J. Biol. Chem. 254*, 3182–3186.

Ho, P. S., Hoffman, B. M., Kang, C. H., & Margoliash, E. (1983) *J. Biol. Chem. 258*, 4356–4363.

Kolthoff, I. M., & Belcher, R. (1957) *Volumetric Analysis*, Vol. III, pp 143–144, Interscience Publishers, Inc., New York.

Kumar, C., Naqui, A., & Chance, B. (1984a) *J. Biol. Chem. 259*, 11688–11671.

Kumar, C., Naqui, A., & Chance, B. (1984b) *J. Biol. Chem. 259*, 2073–2076.

Kumar, C., Naqui, A., Powers, L., Ching, Y.-C., & Chance, B. (1988) *J. Biol. Chem. 263*, 7159–7163.

Lowry, O. H., Rosebrough, N. J., Farr, A. L., & Randall, R. J. (1951) *J. Biol. Chem. 193*, 265–275.

Malmström, B. G. (1990) *Arch. Biochem. Biophys. 280*, 233–241.

McCandlish, E., Miksztal, A. R., Nappa, M., Sprenger, A. Q., & Valentine, J. S. (1980) *J. Am. Chem. Soc. 102*, 4268–4271.

Muijsers, A. O., Tiesjema, R. H., & Van Gelder, B. F. (1971) *Biochim. Biophys. Acta 234*, 481–492.

Orii, Y. (1988) *Ann. N.Y. Acad. Sci. 550*, 105–117.

Orii, Y., & King, T. E. (1976) *J. Biol. Chem. 251*, 7487–7493.

Papadopoulos, P. G., Walter, S. A., Li, J., & Baker, G. M. (1991) *Biochemistry 30*, 840–850.

Vygodina, T. V., & Konstantinov, A. A. (1988) *Ann. N.Y. Acad. Sci. 550*, 124–138.

Wikström, M. (1981) *Proc. Natl. Acad. Sci. U.S.A. 78*, 4051–4054.

Wikström, M. (1987) *Chem. Scr. 27B*, 53–58.

Witt, S. N., & Chan, S. I. (1987) *J. Biol. Chem. 262*, 1446–1448.

Wrigglesworth, J. M. (1984) *Biochem. J. 217*, 715–719.

Yonetani, T. (1960) *J. Biol. Chem. 235*, 3138–3143.

Yonetani, T. (1965) *J. Biol. Chem. 240*, 4509–4514.

Yoshikawa, S., Choc, M. G., O'Toole, M. C., & Caughey, W. S. (1977) *J. Biol. Chem. 252*, 5498–5508.